Connection between Recurrence-Time Statistics and Anomalous Transport

G. M. Zaslavsky[1,2] and Michael K. Tippett[2]

[1]*Space Research Institute, Academy of Sciences of the U.S.S.R., Profsoyuznaya 84/32, Moscow 117810, U.S.S.R.*

[2]*Courant Institute of Mathematical Sciences, New York University, New York, New York 10012*

(Received 3 May 1991)

For a model stationary flow with hexagonal symmetry, we study the recurrence-time statistics. This model flow has been shown elsewhere to provide a sharp transition from normal to anomalous transport. We show here that this transition from normal to anomalous transport is accompanied by a corresponding change of the recurrence-time statistics from "normal" to "anomalous." In the anomalous case the distribution of recurrence times has a power tail. Recurrence-time statistics provide a local measurement to make evident the existence of anomalous transport.

PACS numbers: 47.25.Jn

In this Letter, we examine the chaotic behavior of passive particles in a given velocity field $\mathbf{v}(\mathbf{x},t)$ [1]. The motion of a particle is described by the dynamical system

$$dx/v_x = dy/v_y = dz/v_z = dt\,. \tag{1}$$

For stationary flows, $\mathbf{v}=\mathbf{v}(\mathbf{x})$ and (1) also represents the equations for streamlines. There are applications of (1) to a variety of different practical situations. Also, (1) has been employed in a dynamical systems approach to the fast dynamo problem [2–4] and to the analysis of topological transformations of phase space in the route to turbulence [5–7].

Here we investigate a particular case of the so-called Q flows [5]. These 3D, incompressible flows have the form

$$v_x = -\frac{\partial \psi_q}{\partial y} + \epsilon \sin z,\quad v_y = \frac{\partial \psi_q}{\partial x} + \epsilon \cos z,\quad v_z = \psi_q\,,$$

where

$$\psi_q(x,y) = \sum_{j=1}^{q} A_j \cos(\mathbf{R}\cdot\mathbf{e}_j)$$

and $\mathbf{R}=(x,y)$, $\mathbf{e}_j=[\cos(2\pi j/q),\sin(2\pi j/q)]$ are unit vectors that form a regular q star; A_j are constants, taken here all to be 1. These flows possess the Beltrami property $(\nabla\times\mathbf{v})\times\mathbf{v}=0$. It was shown that the streamlines of the Q flow generate a "stochastic web" with q-fold symmetry [5] in phase space. The case $q=4$ is the ABC flow (Arnold-Beltrami-Childress). In this Letter we investigate the case $q=3$ with hexagonal symmetry. The cases with $q\neq 1,2,3,4,6$ possess quasicrystal symmetry.

In [8], properties of the transport generated by this flow were calculated in the form of asymptotic scaling laws

$$\langle |R(t)| \rangle \sim t^{\mu} \quad (t\to\infty)\,, \tag{2}$$

where $R(t)$ is the displacement of a particle in the (x,y) plane and the averaging is over particles. The case $\mu=0.5$ is considered normal transport in view of its resemblance to Brownian motion. For $0<\mu<0.5$, "captured" particles dominate. For $0.5<\mu<1$, so-called Lévy flights prevail and the transport is referred to as anomalous. The flow that we have chosen to study has the interesting property that there may be normal or anomalous transport depending on the value of ϵ. A critical value of ϵ was found to be $\epsilon_c=2.6$; for $\epsilon\leq\epsilon_c$ there was anomalous diffusion; for $\epsilon\geq\epsilon_c$ there was normal diffusion.

It was found in [8] that bifurcation in the phase portrait accompanies the transition from normal to anomalous transport. This can explain the sharpness of the transition of μ from one value to another. Figure 1 shows the Poincaré section of a streamline by the $z=0$ plane (mod2π) for $\epsilon=2.9$, when there is normal transport ($\mu=0.50$). Figure 1(a) shows the full picture in the (x,y) plane; Fig. 1(b) shows a small part of the (x,y) plane. The domains marked by circles will be described below. Figure 2 shows the same as in Fig. 1(a) for $\epsilon=2.3$, when there is anomalous diffusion ($\mu=0.70$). It is seen in Fig. 2 that in the anomalous regime long regular motion is possible in contrast to the case in Fig. 1(a). Such motion is called a "flight." Huge flights are called "stochastic jets" [5]. Jets appear due to trappings in the boundary layer of nonchaotic islands in the stochastic web. These jets and flights are like Lévy flights for Q flows [8,9]. There are several experimental observations in fluid dynamics of the existence of flights with anomalous passive scalar transport (see, for example, [10]).

The main properties of anomalous transport are reflected in the density probability function $P(R,t)$, which gives the probability of finding a particle at the point R at the moment t. In the case of anomalous transport, $P(R,t)$ has no characteristic scale as in the normal (Gaussian) case and, moreover, divergence of $\langle R^n\rangle$ for $n\geq 2$ indicates a long-tail distribution of $P(R,t)$ [11]. It was shown in [11] that μ is linked to the fractal dimension of the trajectory in space and time. It was also mentioned that a separation of these fractal properties is sometimes impossible, μ being determined by the fractal dimension of both space and time simultaneously [12]. The existence of islands and cantori in real Hamiltonian systems plays a crucial role in determining μ.

Let us look again at (2) in a very general sense. Since it describes a property that holds for large t and $R(t)$, (2) gives a large-scale property of the system. In contrast, the parameter μ comes from the microscopic or local properties of the phase space. The microscopic behavior is described in a geometric way (fractal dimension), which is in some sense physically unobservable whereas

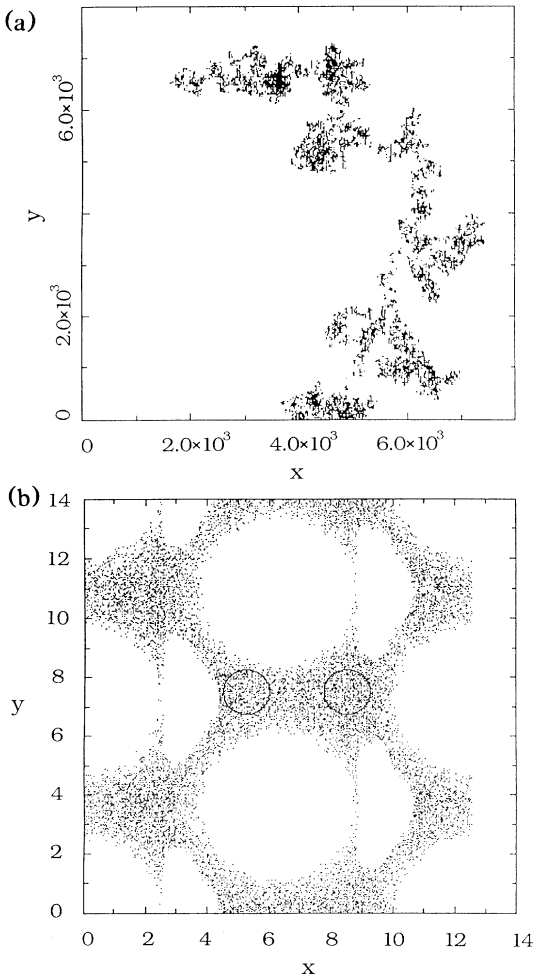

FIG. 1. Poincaré section of the orbits by the plane $z=0(\mathrm{mod}2\pi)$ for $\epsilon=2.9$. (a) The entire plane; (b) a section of size $(4\pi)^2$ for forward crossings only.

the macroscopic diffusion is a fairly explicit process. We would like to be able to observe macroscopic properties from the local measurements of the system. Aside from theoretical interest in being able to do this, there are practical applications. The measurement of Poincaré recurrence times (PRT) does just this.

Consider the motion of a particle in a $4\pi\times4\pi/\sqrt{3}\times2\pi$ box with periodic boundary conditions. The recurrence time T is the time a particle takes to return to a small sphere S. During a single orbit, the particle will return to the sphere S repeatedly. The distribution of those recurrence times is given by the distribution function $f(T)$. We are interested in the asymptotics of $f(T)$ and of its cumulative distribution $F(T)$,

$$F(T)=\int_0^T f(\tau)d\tau\,. \tag{3}$$

We will comment below on the dependence of $f(T)$ on the size and location of S. It will be shown that the normal diffusion ($\epsilon=2.9$) produces a "normal" distribution

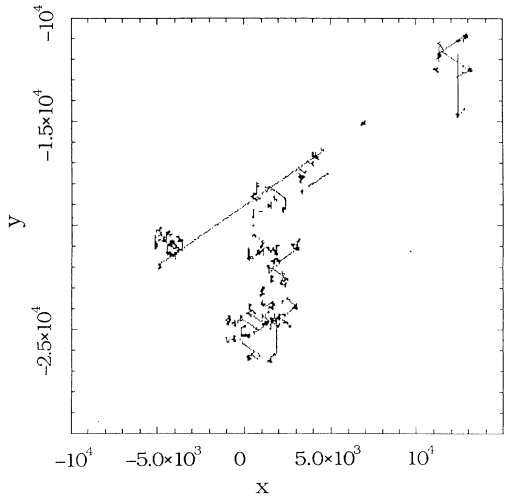

FIG. 2. Poincaré section of the orbits by the plane $z=0(\mathrm{mod}2\pi)$ for $\epsilon=2.3$ for forward and backward crossings.

of PRT times, while the anomalous diffusion ($\epsilon=2.3$) produces an "anomalous" distribution having a power tail.

Consider a simple argument for the form of PRT statistics for the case of normal diffusion. It is known [13] that the number of periodic orbits with period $T_0<T$ is

$$P(T)\sim e^{hT}\,, \tag{4}$$

where h is the Kolmogorov-Sinai entropy. More accurate estimates can be found in [14] and several examples exist in [15]. An important result for the following is the Bowen and Maer theorem [14] on the asymptotic equivalence of averaging over the phase space and over the periodical orbits for K systems:

$$\int\xi(x,y)\rho(x,y)dx\,dy = \lim_{T\to\infty}\frac{1}{\Gamma_A}\sum_{C(T)\in A}\int_{C(T)}\xi(x_c,y_c)dx_c\,dy_c\,, \tag{5}$$

where $\xi(x,y)$ is a physical value at each phase point (x,y), $\rho(x,y)$ is the stationary measure on the phase space, $C(T)$ is a periodic orbit with period T, A is a box of initial conditions with phase volume Γ_A, summing is performed over all periodic orbits belonging to A, and (x_c,y_c) mean that the coordinates (x,y) belong to the periodical orbit C.

Equations (4) and (5) can be used to obtain a qualitative estimate of the probability density $f(T)$ of the first recurrence time T. The set of recurrences to S are all close to the set of periodic orbits that cross S, for large enough T. This allows us to consider the distribution of periodic orbits instead of the quasiperiodical ones which form the set of recurrences to S. In other words, the suggestion is that not only is averaging over periodic orbits equivalent to averaging over stochastic orbits, as stated in

(5), but there is an equivalence between the distributions of periodic orbits and the distribution of quasiperiodic orbits that return to S. Thus,

$$f(T)=(1/\langle T\rangle)\exp(-T/\langle T\rangle), \quad (6)$$

with some constant $\langle T\rangle$, and is consistent with (4). It seems that $\langle T\rangle\sim 1/S$ for small enough S; however, this point is more complicated and will be discussed below. The cumulative distribution function defined by (3) can be found from the normalized probability distribution (6) to be

$$F(T)=1-\exp(-T/\langle T\rangle) \quad (7)$$

with mean recurrence time $\langle T\rangle$.

Let us introduce more rigorous arguments for the formula (7) by considering a simple model mapping $\hat{T}$: $\hat{T}x=Kx \pmod 1$, $x\in(0,1)$, where K is an integer and $K\gg 1$. Consider the interval (0,1) and its partition over subintervals $S_n(j)$:

$$S_n(j)=[j/K^n,(j+1)/K^n] \quad (j=0,\ldots,K^n-1). \quad (8)$$

The length of each subinterval $S_n(j)$ is

$$\Delta_n=K^{-n}. \quad (9)$$

Applying the mapping $\hat{T}$ to $S_n(j)$ yields

$$\hat{T}S_n(j)=[j/K^{n-1},(j+1)/K^{n-1}]=S_{n-1}(j)$$

or

$$\hat{T}^n S_n(j)=(0,1),$$

independently of j.

Choose an initial point of an orbit to be in $S_n(j_0)$ with fixed $j=j_0$. After the first iteration [the first action of the operator $\hat{T}$ on $S_n(j_0)$] all points from $S_n(j_0)$ escape the interval except for a fraction, $1/K$, of them which return to the interval. This property persists for subsequent iterations until the nth iteration when all intervals, S_n, will cover homogeneously the interval (0,1). The remarkable property of this construction is that the first recurrence appears after n iterations with probability $\Delta_n[1-O(1/K)]$. Using formula (9) for Δ_n, one can see that this probability and expression (6) are the same if one takes into account discrete time and adds the normalization constant $\langle T\rangle=1/\ln K$.

There is a simple physical meaning to this result. Because of the mixing property of this chaotic mapping, an orbit is likely to return to the initial volume S in a relatively short time. Thus, because of the mixing, the probability of the first recurrence occurring after a long time should be small. Stated another way, only a very small volume $\Delta_n[1-O(1/K)]$ is filled by such orbits which can avoid recurrences for a long time, $T\gg\langle T\rangle$.

The real situation with Q flows is not so simple as in the above example. Nevertheless, numerical simulation confirms with extremely good accuracy the law (6) for the case of normal diffusion.

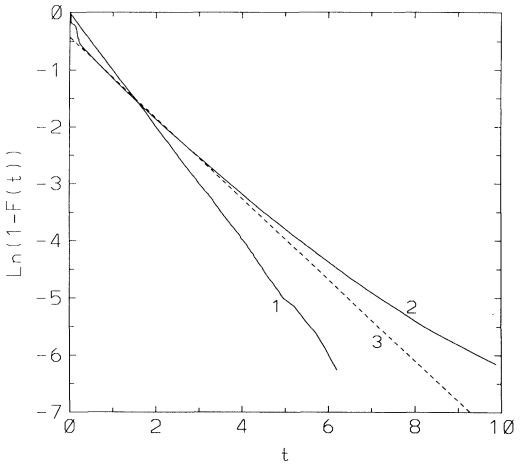

FIG. 3. Poincaré recurrence-time statistics, plot of $\ln[1-F(t)]$ vs t. Curve 1, $\epsilon=2.9$ normal diffusion; curve 2, $\epsilon=2.3$ anomalous diffusion; and curve 3, least-squares fit to curve 2.

To provide the numerical simulation of PRT statistics, particle orbits were calculated for times of order 10^5 (in dimensionless units), using a fourth-order Runge-Kutta method. The general picture of diffusion and mixing is shown in Figs. 1 and 2, where Poincaré sections are displayed. To obtain PRT statistics, different spheres S were taken. Their equatorial sections are shown by circles in Fig. 1(b). By changing the radius of a sphere, the dependence of the PRT statistics on the recurrence volume size may be observed. The size of S should be small enough to avoid the influence of the boundaries of the diffusion area. However, if the volume of S is too small, there are not enough events. The main results of the simulations are shown in Figs. 3 and 4 and in Table I. In Figs. 3 and 4 we use the normalized time $t=T/\langle T\rangle$. The first group of results belongs to the normal diffusion case when $\epsilon=2.9$. Two different domains S (all spheres) are shown in Fig. 1(b). A third sphere was used for orbits crossing the plane $z=0$ in the reverse direction. Coordinates of the centers of S are given in Table I in parentheses. Different radii of the domain are represented in the left column of the table (the maximal radius 0.75 is shown in Fig. 1). It was found that all results for these three domains fit the distribution $f(t)=\exp(-\alpha T/\langle T\rangle)$, where the average $\langle T\rangle$ was obtained directly from the data series and α is a fitting constant. It is seen from the table that for S with a small enough radius there is a confirmation of the exponential law (6) or (7) and α is very close to 1. The value N is the number of events. The influence of the boundaries of chaotic behavior is seen to be stronger for the reverse flow relative to the direction of the z axis (bottom part of Table I). Even very large statistics in the second case shown in the bottom part of Table I give α far from 1. The almost straight line 1 in Fig. 3 corresponds to the second case from the top part of Table I. It confirms the exponential law of PRT distribution.

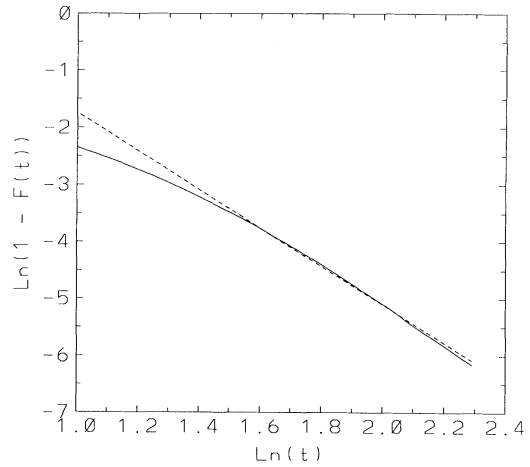

FIG. 4. Poincaré recurrence-time statistics for $\epsilon=2.3$, plot of $\ln[1-F(t)]$ vs $\ln(t)$ with least-squares fit to tail.

The situation in the case of anomalous diffusion ($\epsilon=2.3$) is very different from the normal one. There are more flights than trappings and this property is reflected in the value of $\mu=0.70$ for the law (2). Just this signature should appear in a power tail of the distribution function of periodic orbits and in the PRT distribution

$$f(T)\sim 1/T^{\gamma} \quad (T\to\infty). \tag{10}$$

It is clear that if flights have a finite measure, then the exponential law (7) will hold only for a finite time. After this a crossover to (10) takes place. The data presented in Figs. 3 and 4 show just this result. These data come from PRT statistics of a sphere centered at (5.25,7.5, 0.0) with radius 0.75. We comment below on the results from the other spheres. For small T exponential behavior is seen in curve 2 of Fig. 3; for convenience the best-fit straight line is given (dashed line, labeled 3). For $t\gg 3$ the numerical evidence indicates that the PRT distribution is not exponential. In Fig. 4 the tail of curve 2, $t\gg 3$, is considered. The log-log plot in Fig. 4 suggests a power-law tail corresponding to $\gamma=3.4$ in formula (10). There are 16422 events in this part of the distribution, providing good accuracy of the results and reliability of the crossover from exponential to power law.

The results for other spheres are qualitatively the same; that is, they show a power-tail distribution. However, the exponents γ depend on the choice of domain S and its size. This dependence is not surprising because of the nonhomogeneous character of flights and the transport exponent μ in (2). It seems that the inhomogeneity of γ should appear and an interval of different values of γ is more reasonable than a single value.

One can consider PRT statistics as a local test of large-scale behavior. After a long wandering, particles come back to the domain S, carrying a memory about phase space topologically far from S. This type of testing could appear to be useful when a global experiment is not available.

TABLE I. The main results of the simulations.

Radius	$\langle T\rangle$	α	N
	$(x_0=5.25,y_0=7.5,z_0=0)$		
0.75	259	0.81	24113
0.375	2626	0.99	18372
	$(x_0=8.5,y_0=7.5,z_0=0)$		
0.75	238	0.88	26296
0.375	2581	0.99	18692
	$(x_0=7.25,y_0=3.75,z_0=0)$		
0.75	81	0.49	76694
0.375	349	0.65	138232
0.1875	1787	1.00	13986

The authors thank H. Weitzner for interesting discussions. One of us (G.M.Z.) is appreciative to CIMS for help in organizing and supporting this investigation. This research was funded by U.S. Department of Energy Grant No. DE-FG02-86ER53223.

[1] H. Aref, J. Fluid Mech. **143**, 1 (1984).
[2] V. I. Arnold, *Mathematical Methods in Classical Mechanics* (Springer-Verlag, New York, 1979).
[3] M. Henon, C.R. Acad. Sci. Paris **262**, 353 (1966).
[4] T. Dombre, U. Frisch, J. M. Green, M. Henon, A. Mehr, and A. Soward, J. Fluid Mech. **167**, 102 (1988).
[5] G. M. Zaslavsky, R. Z. Sagdeev, and A. A. Chernikov, Zh. Eksp. Teor. Fiz. **94**, 102 (1988) [Sov. Phys. JETP **67**, 270 (1988)].
[6] A. A. Chernikov, R. Z. Sagdeev, and G. M. Zaslavsky, in *Topological Fluid Dynamics,* edited by H. K. Moffatt and A. Tsinofer (Cambridge Univ. Press, Cambridge, 1990), p. 45.
[7] K. Bajer and H. K. Moffatt, J. Fluid Mech. **212**, 337 (1990).
[8] A. A. Chernikov, B. A. Petrovichev, A. V. Rogal'sky, R. Z. Sagdeev, and G. M. Zaslavsky Phys. Lett. A **144**, 127 (1990).
[9] B. A. Petrovichev, A. V. Rogal'sky, R. Z. Sagdeev, and G. M. Zaslavsky, Phys. Lett. A **150**, 391 (1990).
[10] R. Ramshankar, D. Berlin, and J. P. Gollub, Phys. Fluids A **2**, 1955 (1990).
[11] E. W. Montroll and M. F. Shlesinger, in *Studies in Statistical Mechanics,* edited by J. Lebowitz and E. W. Montroll (North-Holland, Amsterdam, 1984), Vol. 11, p. 5.
[12] Afanas'ev R. Z. Sagdeev and G. M. Zaslavsky, Chaos (to be published).
[13] Ya. G. Sinai, Izv. Akad. Nauk SSSR, Ser. Mat. **30**, 1275 (1966).
[14] R. Bowen and J. Maer, J. Math. **94**, 413 (1972).
[15] G. M. Zaslavsky, *Chaos in Dynamic Systems* (Harwood Academic, New York, 1985).